Formation of Two-Dimensional Complexes of F-Actin and Crosslinking Proteins on Lipid Monolayers: Demonstration of Unipolar α-Actinin-F-Actin Crosslinking

Kenneth A. Taylor and Dianne W. Taylor
Department of Cell Biology, Duke University Medical Center, Durham, North Carolina 27710 USA

ABSTRACT A method is described for forming two-dimensional (2-D) paracrystalline complexes of F-actin and bundling/gelation proteins on positively charged lipid monolayers. These arrays facilitate detailed structural studies of protein interactions with F-actin by eliminating superposition effects present in 3-D bundles. Bundles of F-actin have been produced using the glycolytic enzymes aldolase and glyceraldehyde-3-phosphate dehydrogenase, the cytoskeletal protein erythrocyte adducin as well as smooth muscle α-actinin from chicken gizzard. All of the 2-D bundles formed contain F-actin with a 13/6 helical structure. F-actin-aldolase bundles have an interfilament spacing of 12.6 nm and a superlattice arrangement of actin filaments that can be explained by expression of a local twofold axis in the neighborhood of the aldolase. Well ordered F-actin-α-actinin 2-D bundles have an interfilament spacing of 36 nm and contain crosslinks 33 nm in length angled ~25–35° to the filament axis. Images and optical diffraction patterns of these bundles suggest that they consist of parallel, unipolar arrays of actin filaments. This observation is consistent with an actin crosslinking function at adhesion plaques where actin filaments are bound to the cell membrane with uniform polarity.

INTRODUCTION

Actin filaments form a large number of cytoskeletal structures under the influence of various crosslinking proteins. Actin bundles are closely crosslinked parallel arrays of actin filaments. In vivo actin bundles are found in microvilli, stereocilia, and the acrosomal process among other places. Actin gels are much looser aggregations of randomly oriented filaments that occur as a supporting structure under the plasma membrane. Actin bundles and gels are formed by separate classes of proteins (Pollard and Cooper, 1986), but some proteins are capable of forming both gels and bundles depending on conditions thereby demonstrating that the distinction between gelation protein and bundling protein is not clearly defined.

Many actin binding proteins exhibit bundling activity. Actin bundles in microvilli contain fimbrin (Bretscher and Weber, 1980a) and villin (Bretscher and Weber, 1980b), both of which are actin bundlers but of unrelated structure (de Arruda et al., 1990). Other proteins exhibit bundling activity but are not known to form bundle-like structures in vivo. For example, adducin, which mediates the actin-spectrin interaction in the erythrocyte membrane skeleton, can form tight actin bundles in solution (Misch et al., 1987; Gardner and Bennett, 1987). Various glycolytic enzymes can also form actin bundles in vitro (Morton et al., 1977; Clarke and Morton, 1976; Stewart et al., 1980), but are not known to do so in vivo.

Actin gelation proteins generally are elongated molecules capable of crosslinking actin filaments over long distances. Proteins with F-actin gelation properties include α-actinin (Holmes et al., 1971; Goll et al., 1972), filamin (Wang et al., 1975), spectrin (Bennett, 1985), and ABP-120 (Condeelis et al., 1984). These proteins are all characterized by extended dimeric structures composed of homologous actin binding domains that are separated by pseudorepeats of either α-helical or β-sheet domains (Matsudaira, 1991).

In nearly all instances, F-actin bundles and gels formed in solution are 3-D in character, which makes them difficult objects to analyze by electron microscopy. In addition, some bipolar 3-D bundles constructed from a hexagonal filament arrangement have an intrinsic filament disorder (Francis and DeRosier, 1990). Structural study of these bundles and gels would be greatly facilitated by a method that produced exclusively 2-D bundles. We have previously reported a method to produce large, single-layer paracrystalline arrays of F-actin (Taylor and Taylor, 1992) and have now extended this procedure to incorporate actin bundling proteins into the F-actin array. This method prevents growth of the bundle in the 3rd dimension, thereby facilitating more detailed structural studies on actin-protein interactions than has been possible to this point.

Our preliminary experiments reported here with α-actinin-F-actin bundles show that the chicken gizzard isoform can form bundles of parallel unipolar actin filaments. This is an orientation that could have been predicted based on cellular localization, but which has not previously been demonstrated in vitro. The methodology described here will facilitate detailed structural study of α-actinin-F-actin bundles formed from different muscle and non-muscle isoforms. We believe that the approaches outlined here can be adapted to produce 2-D macromolecular complexes from other systems for structural examination.

Received for publication 13 May 1994 and in final form 5 August 1994.
Address reprint requests to Kenneth A. Taylor, Department of Cell Biology, Duke University Medical Center, Box 3011 Durham, NC 27710–3011. Tel.: 919-684-8961; Fax: 919-684-3687; E-mail: ken_taylor@cellbio.duke.edu.

0006-3495/94/11/1976/08 $2.00

MATERIALS AND METHODS

Protein and lipid preparation

Actin was prepared from rabbit muscle acetone powder as described by Pardee and Spudich (1982) with the modification that the chromatography step was done on a Superose-12 column. G-actin was prepared from F-actin by overnight dialysis at 2°C against buffer A, which consisted of 2 mM Tris-Cl, 0.2 mM Na_2 ATP, 0.02% β-mercaptoethanol, 0.2 mM $CaCl_2$, 0.01% NaN_3, pH 8.0 (at 25°C). The G-actin preparation was clarified immediately before use. Glycolytic enzymes from rabbit muscle were purchased as crystalline suspensions from Sigma Chemical Co. (St. Louis, MO). α-Actinin was prepared according to Feramisco and Burridge (1980). Adducin was prepared according to Gardner and Bennett (1986).

Crystalline suspensions of glycolytic enzymes were dialyzed overnight into a phosphate-free actin binding buffer consisting of 10 mM KCl, 10 mM imidazole, 1 mM EGTA, 2 mM $MgCl_2$, 0.02% β-mercaptoethanol, 0.05% NaN_3, pH 6.0–6.8. They were then diluted into the dialysis buffer to a final protein concentration of 280 μg/ml for glyceraldehyde-3-phosphate dehydrogenase (GPDH) and 300–600 μg/ml for aldolase. Adducin at a concentration of ~250 μg/ml was diluted to a final concentration of 18 μg/ml in the phosphate-free binding buffer.

Lipid layers were prepared on Teflon blocks into which an array of 5 mm diameter × 1 mm deep wells (30 μl volume) had been milled. All lipid layers were prepared by layering 0.5 μg of lipid-surfactant mixture in chloroform on the surface of the crystallizing solution. Lipid layers were prepared from dilauryl phosphatidylcholine (DLPC) (Avanti (Alabaster, AL) or Calbiochem (La Jolla, CA)) and didodecyldimethyl ammonium (DDMA) (Kodak) mixed in the proportions of 70:30 by weight in chloroform.

Formation of 2-D arrays of F-actin and F-actin bundles

Paracrystalline arrays of F-actin were produced as described earlier (Taylor and Taylor, 1992) with 0.25–0.30 μg of G-actin being injected using a Hamilton syringe under the lipid monolayer into a polymerizing buffer. The polymerization is done at 2°C. F-actin crystallization buffers usually consisted of 20–50 mM KCl, 20 mM PO_4, 1 mM ATP, 2 mM $MgCl_2$, 0.02% β-mercaptoethanol, 1 mM EGTA, 0.05% NaN_3, pH 6–7, both with and without 7.5% glycerol (Serva, analytical grade). These F-actin paracrystals are stable for 2–3 months after formation but can be used after 24 h of incubation at 2°C.

The technique for forming 2-D bundles is derived from well established methods for decorating actin filaments with myosin subfragment 1 (Moore et al., 1970). After recovering the actin rafts from the lipid monolayer, the 2-D bundles are produced simply by washing the grid containing the actin paracrystals with a solution of the bundling protein in an appropriate actin binding buffer. Bundles were formed at 2°C by washing the grid with 2–4 drops of the bundling protein, left for 1 min, followed by another 2–4 drops of the bundling protein.

α-Actinin-F-actin 2-D bundles are produced by polymerization of G-actin in the presence of α-actinin. These 2-D bundles will form under a variety of conditions so that the procedure described here is merely a guideline. The conditions that worked best involved premixing the α-actinin with G-actin and then overlaying the mixture with the lipid-surfactant solution in chloroform. Both α-actinin and G-actin were first diluted to 1 μg/μl in buffer A. These proteins were then mixed in different ratios with actin polymerization buffer and ~30 μl of the mixture placed in the Teflon wells. The wells could be sampled within a few hours or left to incubate overnight. Prolonged incubation usually led to the production of α-actinin crystals. The most dependable combination was 16 μg G-actin:30–50 μg α-actinin/ml buffer. As with the formation of F-actin arrays, it seems best to do this polymerization at low temperature to achieve slow filament growth (Kasai, 1969). The binding of α-actinin to F-actin is also higher at low temperature (Goll et al., 1972).

Electron microscopy

Reticulated carbon grids were prepared as described previously (Fukami and Adachi, 1965) with modifications described by Toyoshima (1989). Because that method utilizes surfactant to regulate hole size, we have found it best to remove any trace of surfactant before recovery of the crystals. After stabilizing the reticulated film by vacuum deposition of a heavy layer of carbon, the plastic and surfactant are removed using ethylacetate. This treatment involved placement of the grid into a glass petri dish containing a thin layer of ethyl acetate and a disk of filter paper. Grids were placed on the filter paper, plastic (grid bar) side down, and left for 20 s. The procedure was repeated twice, each time with fresh filter paper and ethylacetate and the grids then air-dried. Film preparations that displayed poor recovery of lipid films were treated repeatedly until their behavior was satisfactory. Actin paracrystals could then be recovered with high efficiency by placing the reticulated carbon grid, carbon side down, onto the lipid monolayer and lifting it after a 5- to 15-min waiting period. Paracrystals can be recovered using continuous carbon support films, but the efficiency is much poorer than can be achieved using reticulated carbon supports and the bundles are more fragmented.

Specimens were stained by washing with 5 drops of an aqueous 2% uranyl acetate solution. When specimens are recovered using reticulated carbon grids, the holes were stabilized by carbon evaporation. Specimens were examined on a Philips EM 301 electron microscope. All micrographs shown here were taken under high dose conditions. Images were screened and optical diffraction patterns recorded using a folded optical diffractometer (Erickson et al., 1978). All dimensions derived from the micrographs are based on the axial spacing of the 5.9-nm actin layer line used as an internal length standard. Helical symmetries are based on the ratio of the axial spacings of the 5.9-nm actin layer line and the first non-equatorial layer line.

RESULTS

We have investigated several approaches of forming 2-D bundles on lipid monolayers, two of which gave the most reproducible results. One of these methods uses 2-D paracrystals of F-actin as a starting material, the other utilizes the polymerization of G-actin in the presence of the bundler. Between these two methods, we have been able to produce 2-D bundles/gels of all the proteins we have tried to date.

Formation of 2-D bundles starting with F-actin paracrystals

Tight 2-D bundles made from globular bundling proteins can be produced starting with 2-D paracrystals of F-actin. Our method for producing F-actin paracrystals generally results in formation of unipolar arrays of filaments (Taylor and Taylor, 1992). This is the preferred orientation of F-actin in many naturally occurring bundles, such as the microvillus (Mooseker and Tilney, 1975) and the acrosome (Tilney et al., 1981). We have formed these bundles using two different glycolytic enzymes as well as the protein adducin.

The literature on glycolytic enzyme-F-actin bundles contains no example of clearly 2-D bundle formation. Bundles formed from aldolase and GPDH using the methods described here were characterized as extensive 2-D arrays which are coherent over areas sometimes as large a 1 μm^2 (Fig. 1 *A*). We have had most of our experience using aldolase, so that those bundles are the best ordered examples shown. Optical diffraction of the aldolase-actin bundle consists of sharp spots that display a superlattice. The actin filaments in this bundle have 13/6 helical symmetry. The interfilament spacing is 12.6 nm. Rabbit muscle aldolase is a tetramer with dimensions of 9.0 nm × 9.0 nm × 6.5 nm (Sygusch et al., 1985), so that this spacing would be

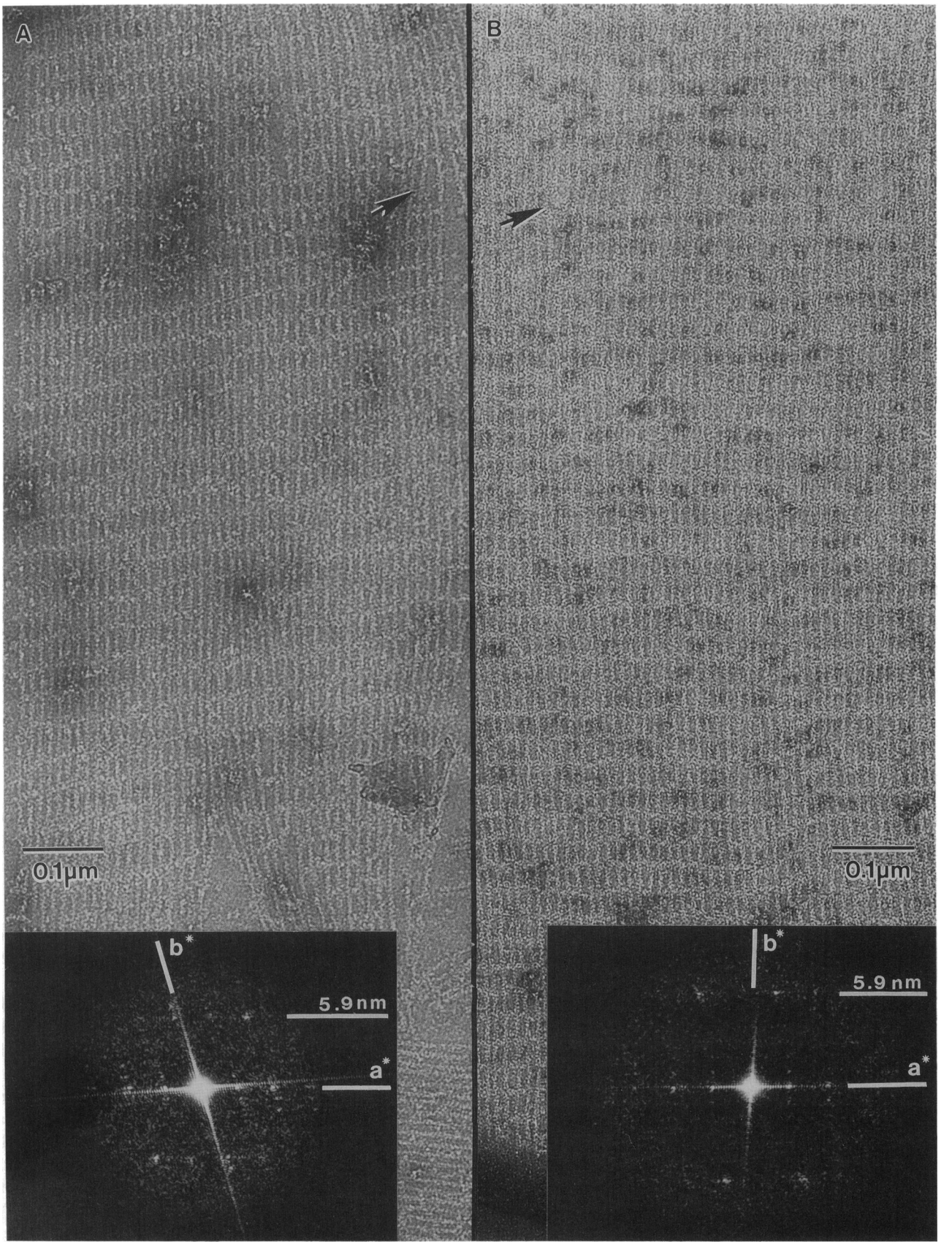
A
0.1μm
b*
5.9nm
a*
B
0.1μm
b*
5.9nm
a*

compatible with the short axis of the tetramer lying within the plane of the 2-D array.

The formation of a superlattice can be explained by the internal symmetry of the bundling protein. Both of the glycolytic enzymes tested have 222 or near 222 symmetry (Sygusch et al., 1987; Gamblin et al., 1990; Rossman et al., 1972). Expression of this symmetry in the immediate environment of the bundling protein would result in the two actin monomers on adjacent filaments bound to the aldolase being related by a local twofold axis oriented parallel with the filament axis. This local twofold axis will cause an axial displacement of 2.75 nm, which is approximately the same as a 180° azimuthal rotation, between adjacent actin filament. The effect, however, is to produce slightly different crosslinking environments for the aldolase across the superlattice period of 2-D bundle.

The procedure of washing the actin rafts with the bundling protein solves any problems that might arise due to incompatibility between conditions used for actin polymerization and conditions that are favorable for actin binding. Actin rafts are best produced in phosphate buffer. However, both phosphate and ATP are strong inhibitors of aldolase binding to F-actin (Arnold and Pette, 1970), and we failed to form actin-aldolase bundles in the actin polymerization buffer.

The formation of 2-D adducin bundles followed the same pattern as the glycolytic enzyme bundles (Fig. 1 *B*). Adducin is a tetramer consisting of two α-subunits, M_r 81 kDa, and two β-subunits, M_r 80 kDa (Joshi et al., 1991). Adducin is an overall acidic protein with a 39-kDa globular domain and an extended tail segment of ~41 kDa (Joshi and Bennett, 1990; Joshi et al., 1991). The tail segment has regions that are both highly acidic and highly basic. Although the presence of a twofold symmetry axis in the tetramer has yet to be demonstrated, the bundles formed nevertheless displayed a similar pattern in projection as those formed using the glycolytic enzymes. Interestingly, the globular headpiece, clearly observed between the actin filaments, apparently lacks actin binding activity on its own (Joshi and Bennett, 1990). The size of the arrays produced here (of which Fig. 1 *B* is only a part) considerably dwarf those in published micrographs of adducin-F-actin bundles which reveal an area of 2-D bundled filaments from a 3-D bundle that is 7 filaments wide and only 320 nm in length (Misch et al., 1987).

There is much less information available on the dimensions of adducin than there is for the glycolytic enzymes, so that interpretation of these images is difficult. Images of negatively stained adducin molecules reveal molecules 10–12 nm in diameter (Gardner and Bennett, 1986), dimensions that are assumed to represent those of tetramers. The interfilament spacing in the adducin-F-actin arrays is 14.5 nm, which is too short to accommodate the globular headpiece between the filaments. Even the more realistic dimension of 8.9 nm for adducin tetramers based on mass and hydrated protein volume (Joshi et al., 1991) is too large to be accommodated between the filaments suggesting that adducin may be positioned above the actin filaments. Substantially more work needs to be done to explain the F-actin-adducin bundles.

The degree of success in forming 2-D bundles under different conditions suggests limits on the affinity that the bundler must have to form the paracrystalline array. The K_d for the aldolase-actin complex is ~8 nM at low ionic strength in the absence of phosphate and ATP but ~200 μM in 10 mM phosphate or 1 mM ATP (Arnold and Pette, 1970), which is so low that incorporation into the actin rafts does not occur. The highest reported K_d for the adducin-F-actin complex is 28 μM (Gardner and Bennett, 1987; but see also Misch et al., 1987) which suggests a lower limit on the affinity that can lead to formation of the 2-D bundles.

The use of a solution with a high concentration of bundling protein or excessive washing of the F-actin rafts with the bundling protein can sometimes "lift" the actin raft off of the lipid monolayer. This happened less often with aldolase and GPDH and was more of a problem with adducin, which is the largest of the bundlers tested (M_r 322 kDa). The glycolytic enzymes, which are basic proteins (Malamud and Drysdale, 1978), presumably alter the electrostatic charge of the actin filament (a strongly acidic protein), which is largely responsible for binding to the lipid monolayer. The effect in adducin may be due to the basic carboxyl terminal domain (Joshi et al., 1991).

Formation of 2-D bundles through G-actin polymerization

The method described above for tight bundle formation seems to be poorly adapted for use with large gelation proteins such as α-actinin. Presumably these large proteins with widely separated actin binding domains are unable to work themselves between the tightly packed actin filaments. In this case, we have found that polymerization of G-actin in the presence of the gelation protein can produce a 2-D array. The method seems to work best when the gelation protein binds to the lipid monolayer with high affinity, which is the case with α-actinin. It has not worked with the glycolytic enzymes, which are basic proteins and do not partition to the positively charged monolayer.

FIGURE 1 Electron micrographs of 2-D F-actin bundles formed on 30:70 DDMA-DLPC lipid layers. (*A*) F-actin-aldolase bundle with optical diffraction pattern shown in the insert. The unit cell is a superlattice which can be seen by the lack of intersection of a line drawn through the clusters of spots on the equator with a similar line drawn through the corresponding clusters of spots centered on the 5.9-nm layer line. The superlattice is not unique, just as the superlattices found in the starting actin rafts are not unique. The arrowhead in the upper right hand corner points to an actin filament that ends but where further along the paracrystal, crosslinking continues between its two neighboring filaments. This supports the conclusion that the actin filaments in the rafts are in the parallel orientation. (*B*) F-actin-adducin bundle with associated diffraction pattern shown in the insert. The actin filaments in both the aldolase and adducin bundles show a helical symmetry of 13/6. The globular head piece of adducin that separates the actin filaments is best seen in the lower part of the figure where the stain layer is heaviest. The arrow in the upper left hand corner points to a discontinuity in the raft similar to that in *A* that helps establish the polarity of the bundle.

Typical α-actinin-F-actin arrays formed by this method consisted of 4–10 filaments heavily crosslinked by ~2 α-actinins per crossover repeat (Fig. 2 *A, C, D*). These arrays were rarely as well ordered as the tight bundles but in some cases were sufficiently well ordered to give rise to sampled optical diffraction patterns (Fig. 2 *B*). The improvements obtained by our procedure is evident after comparison with published examples of gels formed in solution. We surveyed three references showing high resolution electron micrographs of α-actinin-F-actin gels (Podlubnaya et al., 1975; Endo and Masaki, 1982; Meyer and Aebi, 1990) but found no examples of ordered 2-D gels as many as 3 actin filaments wide. The method described here produces arrays that wide by default and often results in arrays that are considerably wider and longer.

The 2-D bundles reveal several new characteristics of α-actinin-F-actin bundles. The diffraction pattern (Fig. 2 *B*) indicates an interfilament spacing of 36 nm, a crossover spacing of 35.4 nm, and a helical symmetry of 13/6 for the actin filaments. In regions of straight bundles, the α-actinin crosslinks are always angled ~25–35° relative to the filament axis. The length of the crosslinker can then be estimated at 33 nm after accounting for the 9-nm diameter of the actin filament (Holmes et al., 1990). This length is compatible with the 34-nm length of α-actinin molecules derived from 2-D crystals formed on lipid monolayers (Taylor and Taylor, 1993). The length of the crosslinks also indicates that the α-actinin interaction with F-actin must be occurring at the very ends of the molecule, since there is very little length to spare for extensive overlap.

The orientation of the actin filaments in these 2-D bundles can be ascertained from the images themselves, the majority of which have crosslinks with a single orientation. This suggests that the actin filaments in the bundles have the same orientation. Bundles with bipolar actin filaments would reveal alternating orientations for the crosslinks. The orientation of the filaments can more objectively be determined from the optical diffraction pattern provided that the images have sufficient resolution to detect actin polarity. Actin polarity in isolated filaments can usually be determined unambiguously as long as the 5.9- and 5.1-nm layer lines are present, which is the case in the bundles. The strong sampling on both the equatorial and nonequatorial layer lines indicates a well ordered arrangement of actin filaments and crosslinkers. The unit cell is only large enough to contain one actin filament which indicates that the actin filaments in the bundles have the same polarity. A bundle formed from actin filaments with alternating polarity would reveal systematic absences in the equator. A bundle formed from actin filaments with random polarity would reveal a 5.9-nm layer line with little or no sampling. We conclude that the conditions investigated by us so far produce unipolar actin bundles.

DISCUSSION

Utility of lipid monolayers for study of complex structures

Lipid layer crystallization has been used extensively for forming large 2-D arrays of soluble proteins suitable for electron microscopic examination (Uzgiris and Kornberg, 1983). The method requires that proteins bind to the lipid monolayer with high affinity via any of several methods including protein-ligand interactions (Ribi et al., 1988; Robinson et al., 1988), through mediation by inorganic ions (Mosser et al., 1991; Newman et al., 1989), or by nonspecific charge interactions (Darst et al., 1988; Taylor and Taylor, 1993; Schnyder et al., 1994). Often large coherent crystals several square micrometers in diameter are formed that are suitable for a 3-D structure determination at moderate resolution.

The use of lipid monolayers as a substrate for forming large multicomponent complexes into 2-D arrays for electron microscopy has not been explored to the same extent as crystallization. The method has great potential because of the utility of electron microscopy for visualizing large complex structures. In some cases interactions can be visualized at near atomic resolution with moderate resolution 3-D image reconstructions if the atomic structure of the individual components is known (Rayment et al., 1993; Stewart et al., 1993).

The demonstration here of using lipid monolayers to produce 2-D actin bundles has potentially wider application for visualizing interactions in other systems. The purpose of this preliminary communication is to demonstrate the potential of using lipid layer technology for the study of protein interactions and to suggest the possibility that complex structures may be assembled in a systematic fashion for structural study using this method. Cocrystallization is a considerably more difficult problem than crystallization of a pure protein alone, especially when the affinity between the two proteins is low. For two proteins to interact, their individual concentrations must be comparable to the dissociation constant of the complex. Many significant protein interactions occur with dissociation constants of the order of 1–10 μM. Often these interactions are stabilized by additional proteins that target the constituent molecules to particular structures, such as membranes or the myofilament lattice, that maintain a high local concentration. In vitro assembly of the structure, such as an actin bundle or gel, often results in a complex 3-D arrangement that makes visualization of the individual interactions very difficult. Even a protein the size of α-actinin can attain μM concentrations on lipid monolayers (its concentration in the 2-D crystals is ~0.7 μM) so that a high local concentration in the 2-D phase can be achieved without resorting to high concentrations in the bulk phase. This partitioning of the protein components to the 2-D lipid phase facilitates interaction but limits growth perpendicular to the monolayer. Thus, binary and ternary complexes produced on lipid monolayers may function as 2-D analogs of a complex 3-D structure and serve as a vehicle for determining the spatial arrangements of the constituents using electron microscopy. The assembly of 2-D α-actinin-F-actin bundles starting from a mixture of the separate proteins demonstrates that assembly of a 2-D analog of a complex 3-D structure is possible.

The utility of lipid layers for the formation of these 2-D actin bundles lies in the fluidity of the monolayer itself. Actin filaments in rafts bound to a rigid carbon film will not readily separate and allow the bundling protein to intercalate between them. The fluidity of the lipid monolayer facilitates

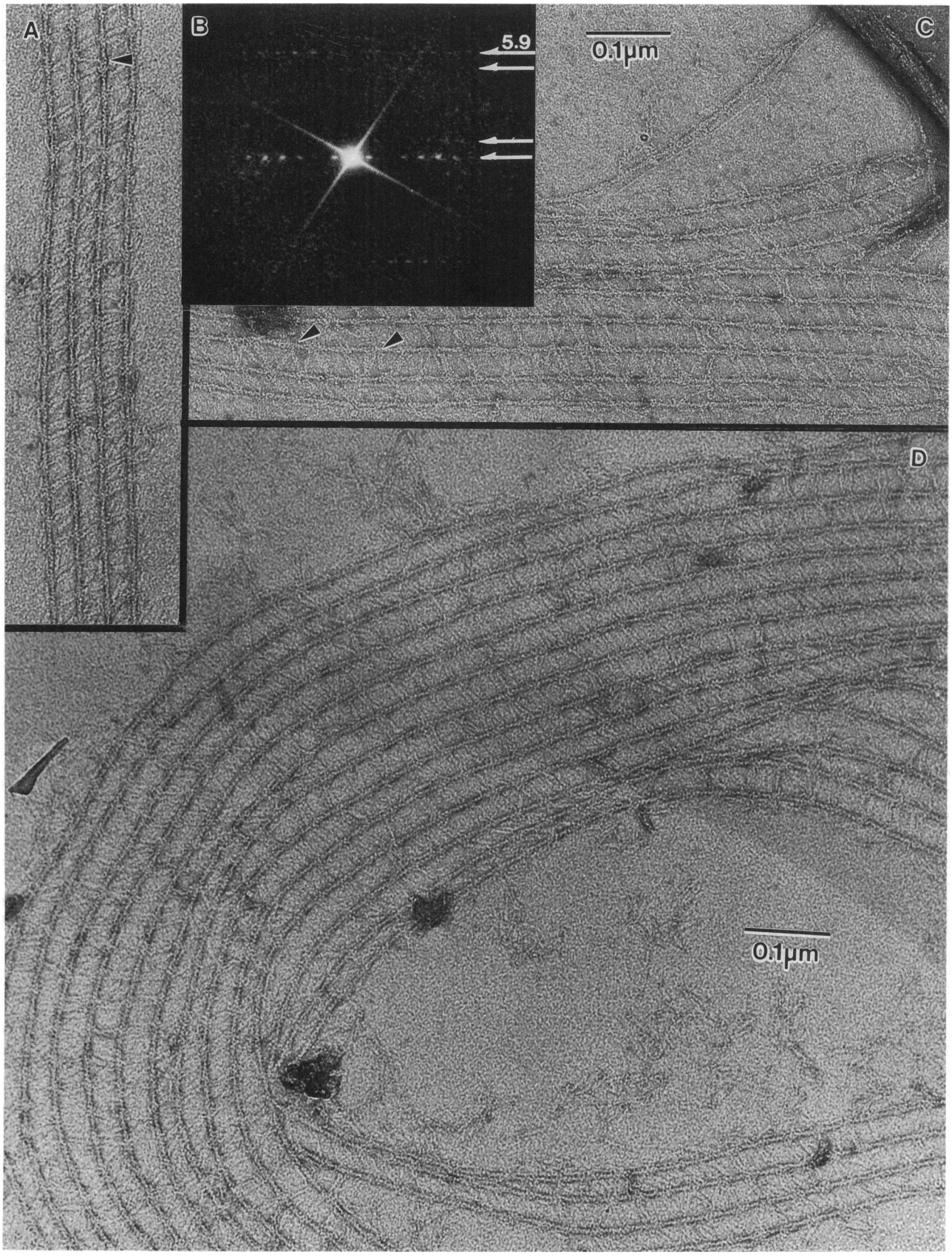

FIGURE 2 F-actin-α-actinin 2-D bundles. (*A*) A particularly well ordered array revealing α-actinin crosslinks angled predominately in one orientation. (*B*) Optical diffraction pattern taken from this same area. The spacing of spots on the equatorial layer line and the spacing of spots on the 5.9-nm layer line is the same indicating that the actin filaments are oriented in the parallel orientation. (*C, D*) Large arrays of F-actin-α-actinin. Arrowheads in *A* and *C* indicate apparent crosslinks angled opposite the predominant orientation. The curved bundle in *D* is not unusual.

intercalation of the bundling protein into the F-actin rafts. In the case of the α-actinin-actin bundles, presumably crosslinking of short actin filaments occurs on the monolayer with elongation continuing after the bundles have first formed. This circumvents the problem of orienting long, preformed actin filaments on the monolayer.

Structure of 2-D bundles of α-actinin and F-actin

The experiments with α-actinin-F-actin bundles produced aggregates that were sufficiently well ordered that the polarity of the actin filaments could be ascertained by optical diffraction. The demonstration that the actin filaments in this structure have the same polarity contradicts the earlier demonstration that the chicken gizzard isoform is an antiparallel actin bundler (Meyer and Aebi, 1990).

There are, however, several reasons to believe that α-actinin isoforms differ in the specificity and orientation of their actin filament crosslinks. In particular, chicken gizzard α-actinin may crosslink both parallel and antiparallel actin filaments. First, in smooth muscle, α-actinin is localized to both adhesion plaques and cytoplasmic dense bodies (Schollmeyer at al., 1976; Geiger et al., 1981; but see also Small, 1985). Adhesion plaques are sites where actin filaments bind to the cell membrane, whereas cytoplasmic dense bodies are anchoring points for antiparallel actin filaments (Bond and Somlyo, 1982; Tsukita et al., 1983). Since actin filaments typically originate from cell membranes in a unipolar orientation (Mooseker and Tilney, 1975; Begg et al., 1978; Small et al., 1978), if α-actinin localized to these regions is functioning as an actin filament crosslinker, it would have to be crosslinking unipolar filaments. Second, skeletal muscle I-segments treated with high salt to remove tropomyosin (an inhibitor of α-actinin binding) bind chicken gizzard α-actinin throughout their length, an observation that has been attributed to self-association of α-actinin molecules (Sanger et al., 1984), but which nevertheless can be interpreted as unipolar crosslinking. Indeed, the arrays produced here seem to have at least 2 α-actinins per crosslink, suggesting that α-actinin self association plays a role in forming these bundles. Third, in striated muscle α-actinin is found in the Z-disks (Masaki et al., 1967; Lazarides and Granger, 1978) but not in the terminal segments (myotendinous junction) of frog skeletal muscle where actin filaments are attached to the cell membrane (Tidball, 1987). Although it has not been demonstrated in vitro that skeletal muscle α-actinin is a bundler of antiparallel actin filaments, its presence in the Z-disk and absence in the terminal segment could suggest a pronounced tendency to bundle antiparallel actin filaments. Finally, in the body wall muscle of the nematode, a 107-kDa protein immunologically related to α-actinin is localized to dense bodies (functional homologues of Z-disks) but not to adhesion plaques of the same fibrils (Francis and Waterston, 1985). The differing distributions of α-actinin in skeletal and smooth muscle could be interpreted as differences in actin crosslinking specificity.

The methods described here make it possible to obtain more detailed information on the structure of F-actin bundles in vitro. Although the clear demonstration of unipolar actin crosslinking for chicken gizzard α-actinin in vitro is surprising, the observation can be refined by repeating the experiment with isoforms isolated from other muscle and nonmuscle sources. Further work is also needed, in particular to determine conditions that might produce bundles of bipolar actin filaments using chicken gizzard α-actinin. An isoform dependent crosslinking specificity would add another dimension to the properties of α-actinin beyond the differing effects of Ca^{2+} on actin filament gelation (Burridge and Feramisco, 1981).

The actin bundles shown here are a limited sample of how a lipid monolayer might be used to produce a 2-D specimen of a complex structure for microscopic examination. Many other possible interactions could be examined in analogous fashion thereby enabling complex structures to be studied by assembly of binary and possibly ternary complexes into 2-D arrays.

We acknowledge the assistance of Drs. Christine Hughes and Vann Bennett (Duke University) with the column purification of actin and the gift of adducin, Dr. Steven Rosenfeld (University of Alabama) for the gift of rabbit muscle acetone powder, and Dr. Keith Burridge (University of North Carolina) for providing α-actinin. The technical assistance of Melody Rice is gratefully acknowledged.

This work was supported by a grant from the American Heart Association and by National Institutes of Health grant GM30598.

REFERENCES

Arnold, H., and D. Pette. 1970. Binding of aldolase and triosephosphate dehydrogenase to F-actin and modification of catalytic properties of aldolase. *Eur. J. Biochem.* 15:360–366.

Begg, D. A., R. Rodewald, and L. I. Rebhun. 1978. The visualization of actin filament polarity in thin sections. Evidence for the uniform polarity of membrane-associated filaments. *J. Cell Biol.* 79:846–852.

Bennett, V. 1985. The membrane skeleton of human erythrocytes and its implications for more complex cells. *Annu. Rev. Biochem.* 54:273–304.

Bond, M., and A. V. Somlyo. 1982. Dense bodies and actin polarity in vertebrate smooth muscle. *J. Cell Biol.* 95:403–413.

Bretscher, A., and K. Weber. 1980a. Fimbrin, a new microfilament-associated protein present in microvilli and other cell surface structures. *J. Cell Biol.* 86:335–340.

Bretscher, A., and K. Weber. 1980b. Villin is a major protein of the microvillus cytoskeleton which binds both G and F-actin in a calcium-dependent manner. *Cell.* 20:839–847.

Burridge, K., and J. R. Feramisco. 1981. Non-muscle α-actinins are calcium-sensitive actin-binding proteins. *Nature.* 294:565–567.

Clarke, F. M., and D. J. Morton. 1976. Aldolase binding to actin-containing filaments. Formation of paracrystals. *Biochem. J.* 159:797–798.

Condeelis J., M. Vahey, J. M. Carboni, J. DeMey, and S. Ogihara. 1984. Properties of the 120,000- and 95,000-dalton actin-binding proteins from *Dictyostelium discoideum* and their possible functions in assembling the cytoplasmic matrix. *J Cell Biol.* 99:119–126.

Darst, S. A., H. O. Ribi, D. W. Pierce, and R. D. Kornberg. 1988. Two-dimensional crystals of *Escherichia coli* RNA polymerase holoenzyme on positively charged lipid layers. *J. Mol. Biol.* 203:269–273.

de Arruda, M. V., S. Watson, C.-H. Lin, J. Leavitt, and P. Matsudaira. 1990. Fimbrin is a homologue of the cytoplasmic phosphoprotein plastin and has domains homologous with calmodulin and actin gelation proteins. *J. Cell Biol.* 111:1069–1079.

Endo, T., and T. Masaki. 1982. Molecular properties and functions in vitro of chicken smooth-muscle α-actinin in comparison with those of striated-muscle α-actinins. *J. Biochem.* 92:1457–1468.

Erickson, H. P., W. A. Voter, and K. Leonard. 1978. Image reconstruction in electron microscopy: enhancement of periodic structure by optical filtering. *Methods Enzymol.* 49:39–63.

Feramisco, J. R., and K. Burridge. 1980. A rapid purification of α-actinin, filamin and a 130,000-dalton protein from smooth muscle. *J. Biol. Chem.* 255:1194–1199.

Francis, G. R., and R. H. Waterston. 1985. Muscle organization in *Caenorhabditis elegans*: localization of proteins implicated in thin filament attachment and I-band organization. *J. Cell Biol.* 101:1532–1549.

Francis, N., and D. J. DeRosier. 1990. A polymorphism peculiar to bipolar actin bundles. *Biophys. J.* 58:771–776.

Fukami, A., and K. J. Adachi. 1965. A new method of preparation of a self-perforated micro plastic grid and its application (I). *J. Electron Microsc.* 14:112–118.

Gamblin, S. J., B. Cooper, J. R. Millar, G. J. Davies, J. A. Littlechild, and H. C. Watson. 1990. The crystal structure of human muscle aldolase at 3.0 Å resolution. *FEBS Lett.* 262:282–286.

Gardner, K., and V. Bennett. 1986. A new erythrocyte membrane associated protein with calmodulin binding activity. *J. Biol. Chem.* 261:1339–1348.

Gardner, K., and V. Bennett. 1987. Modulation of spectrin-actin assembly by erythrocyte adducin. *Nature.* 328:359–362.

Geiger, B., A. H. Dutton, K. T. Tokuyasu, and S. J. Singer. 1981. Immunoelectron microscope studies of membrane-microfilament interactions: distributions of α-actinin, tropomyosin, and vinculin in intestinal epithelial brush border and chicken gizzard smooth muscle cells. *J. Cell Biol.* 91:614–628.

Goll, D. E., A. Suzuki, J. Temple, and G. R Holmes. 1972. Studies on purified α-actinin. I. Effect of temperature and tropomyosin on the α-actinin/F-actin interaction. *J. Mol. Biol.* 67:469–488.

Holmes, G. R., D. E. Goll, and A. Suzuki. 1971. Effect of α-actinin on actin viscosity. *Biochim. Biophys. Acta.* 253:240–253.

Holmes, K. C., D. Popp, W. Gebhard, and W. Kabsch. 1990. Atomic model of the actin filament. *Nature.* 347:44–49.

Joshi, R., and V. Bennett. 1990. Mapping the domain structure of human erythrocyte adducin. *J. Biol. Chem.* 265:13130–13136.

Joshi, R., D. G. Gilligan, E. Otto, T. McLaughlin, and V. Bennett. 1991. Primary structure and domain organization of human alpha and beta adducin. *J. Cell Biol.* 115:665–675.

Kasai, M. 1969. Thermodynamical aspect of G-F transformations of actin. *Biochim. Biophys. Acta.* 180:399–409.

Lazarides, E., and B. L. Granger. 1978. Fluorescent localization of membrane sites in glycerinated chicken skeletal muscle fibers and the relationship of these sites to the protein composition of the Z disc. *Proc. Natl. Acad. Sci. USA.* 75:3683–3687.

Malamud, D., and J. W. Drysdale. 1978. Isoelectric points of proteins: a table. *Anal. Biochem.* 86:620–647.

Masaki, T., M. Endo, and S. Ebashi. 1967. Localization of the 6S component of α-actinin in the Z-band. *J. Biochem. (Tokyo).* 62:630–632.

Matsudaira, P. 1991. Modular organization of actin crosslinking proteins. *Trends Biol. Sci.* 16:87–92.

Meyer, R. K., and U. Aebi. 1990. Bundling of actin filaments by α-actinin depends on its molecular length. *J. Cell Biol.* 110:2013–2024.

Misch, S. M., M. S. Mooseker, and J. S. Morrow. 1987. Erythrocyte adducin: a calmodulin-regulated actin-bundling protein that stimulates spectrin-actin binding. *J. Cell Biol.* 105:2837–2845.

Moore, P. B., H. E. Huxley, and D. J. DeRosier. 1970. Three-dimensional reconstruction of F-actin, thin filaments and decorated thin filaments. *J. Mol. Biol.* 50:279–295.

Mooseker, M. S., and L. G. Tilney. 1975. Organization of an actin-filament-membrane complex: filament polarity and membrane attachment in the microvilli of intestinal epithelial cells. *J. Cell Biol.* 67:725–743.

Morton, D. J., F. M. Clarke, and C. J. Masters. 1977. An electron microscope study of the interaction between fructose diphosphate aldolase and actin-containing filaments. *J. Cell Biol.* 74:1016–1023.

Mosser, G., C. Ravanat, J. M. Freyssinet, and A Brisson. 1991. Sub-domain structure of lipid-bound annexin-V resolved by electron image analysis. *J. Mol. Biol.* 217:241–245.

Newman, R., A. Tucker, C. Ferguson, D. Tsernoglou, K. Leonard, and M. J. Crumpton. 1989. Crystallization of p68 on lipid monolayers and as three-dimensional single crystals. *J. Mol. Biol.* 206:213–219.

Pardee, J. D., and J. A. Spudich. 1982. Purification of muscle actin. *Methods Enzymol.* 85:164–181.

Podlubnaya, Z. A., L. A. Tskhovrebova, M. M. Zaalishvili, and G. A. Stefanenko. 1975. Electron microscopic study of α-actinin. *J. Mol. Biol.* 92:357–359.

Pollard, T. D., and J. A. Cooper. 1986. Actin and actin-binding proteins. A critical evaluation of mechanisms and functions. *Annu. Rev. Biochem.* 55:987–1035.

Rayment, I., H. M. Holden, M. Whittaker, C. B. Yohn, M. Lorenz, K. C. Holmes, and R. A. Milligan. 1993. Structure of the actin-myosin complex and its implications for muscle contraction. *Science.* 261:58–65.

Ribi, H. O., D. S. Ludwig, K. L. Mercer, G. K. Schoolnik, and R. D. Kornberg. 1988. Three-dimensional structure of cholera toxin penetrating a lipid membrane. *Science.* 239:1272–1276.

Robinson, J. P., M. F. Schmid, D. G. Morgan, and W. Chiu. 1988. Three-dimensional structural analysis of tetanus toxin by electron crystallography. *J. Mol. Biol.* 200:367–375.

Rossmann, M. G., G. C. Ford, H. C. Watson, and L. J. Banaszak. 1972. Molecular symmetry of glyceraldehyde-3-phosphate dehydrogenase. *J. Mol. Biol.* 64:237–245.

Sanger, J. W., B. Mittal, and J. M. Sanger. 1984. Analysis of myofibrillar structure and assembly using fluorescently labeled contractile proteins. *J. Cell Biol.* 98:825–833.

Schnyder, T., M. Cyrklaff, K. Fuchs, and T. Wallimann. 1994. Crystallization of mitochondrial creatin kinase on negatively charged lipid layers. *J. Struct. Biol.* 112:136–147.

Schollmeyer, J. E., L. T. Furcht, D. E. Goll, R. M. Robson, and M. H. Stromer. 1976. Localization of contractile proteins in smooth muscle cells and in normal and transformed fibroblasts. *In* Cell Motility, Vol. A. R. Goldman, T. Pollard, and J. Rosenbaum, editors. Cold Spring Harbor Laboratory, Cold Spring Harbor, New York. 361–388.

Small, J. V. 1985. Geometry of actin-membrane attachments in the smooth muscle cell: the localization of vinculin and α-actinin. *EMBO J.* 4:45–49.

Small, J. V., G. Isenberg, and J. E. Celis. 1978. Polarity of actin at the leading edge of cultured cells. *Nature.* 272:638–639.

Stewart, M., D. J. Morton, and F. M. Clarke. 1980. Interaction of aldolase with actin-containing filaments. *Biochem. J.* 186:99–104.

Stewart, P. L., S. D. Fuller, and R. M. Burnette. 1993. Difference imaging of adenovirus: bridging the resolution gap between x-ray crystallography and electron microscopy. *EMBO J.* 12:2589–2599.

Sygusch, J., D. Beaudry, and M. Allaire. 1987. Molecular architecture of rabbit skeletal muscle aldolase at 2.7 Å resolution. *Proc. Natl. Acad. Sci. USA.* 84:7846–7850.

Sygusch, J., H. Boulet, and D. Beaudry. 1985. Structure of rabbit muscle aldolase at low resolution. *J. Biol. Chem.* 260:15286–15290.

Taylor, K. A., and D. W. Taylor. 1992. Formation of 2-D paracrystals of F-actin on phospholipid layers mixed with quaternary ammonium surfactants. *J. Struct. Biol.* 108:140–147.

Taylor, K. A., and D. W. Taylor. 1993. Projection image of smooth muscle α-actinin from 2-D crystals formed on positively charged lipid layers. *J. Mol. Biol.* 230:196–205.

Tidball, J. G. 1987. Alpha-actinin is absent from the terminal segments of myofibrils and from subsarcolemmal densities in frog skeletal muscle. *Exp. Cell Res.* 170:469–82.

Tilney, L. G., E. M. Bonder, and D. J. DeRosier. 1981. Actin filaments elongate from their membrane-associated ends. *J. Cell Biol.* 90:485–494.

Toyoshima, C. 1989. On the use of holey grids in electron crystallography. *Ultramicroscopy.* 30:439–444.

Tsukita, S., S. Tsukita, and H. Ishikawa. 1983. Association of actin and 10 nm filaments with the dense body in smooth muscle cells of the chicken gizzard. *Cell Tissue Res.* 229:233–242.

Uzgiris, E. E., and R. D. Kornberg. 1983. Two-dimensional crystallization technique for imaging macromolecules, with application to antigen-antibody-complement complexes. *Nature.* 301:125–129.

Wang, K., J. Ash, and S. Singer. 1975. Filamin, a new high-molecular-weight protein found in smooth muscle and non-muscle cells. *Proc. Natl. Acad. Sci. USA.* 72:4483–4486.